



**University of
Zurich**^{UZH}

**Zurich Open Repository and
Archive**

University of Zurich
University Library
Strickhofstrasse 39
CH-8057 Zurich
www.zora.uzh.ch

Year: 2009

The SPTLC3 subunit of serine palmitoyltransferase generates short chain sphingoid bases

Hornemann, Thorsten ; Penno, A ; Rütli, M F ; Ernst, D ; Kivrak-Pfiffner, Fatma ; Rohrer, L ; von Eckardstein, Arnold

Abstract: The enzyme serine palmitoyltransferase (SPT) catalyzes the rate-limiting step in the de novo synthesis of sphingolipids. Previously the mammalian SPT was described as a heterodimer composed of two subunits, SPTLC1 and SPTLC2. Recently we identified a novel third SPT subunit (SPTLC3). SPTLC3 shows about 68% identity to SPTLC2 and also includes a pyridoxal phosphate consensus motif. Here we report that the overexpression of SPTLC3 in HEK293 cells leads to the formation of two new sphingoid base metabolites, namely C(16)-sphinganine and C(16)-sphingosine. SPTLC3-expressing cells have higher in vitro SPT activities with lauryl- and myristoyl-CoA than SPTLC2-expressing cells, and SPTLC3 mRNA expression levels correlate closely with the C(16)-sphinganine synthesis rates in various human and murine cell lines. Approximately 15% of the total sphingolipids in human plasma contain a C(16) backbone and are found in the high density and low density but not the very low density lipoprotein fraction. In conclusion, we show that the SPTLC3 subunit generates C(16)-sphingoid bases and that sphingolipids with a C(16) backbone constitute a significant proportion of human plasma sphingolipids.

DOI: <https://doi.org/10.1074/jbc.M109.023192>

Posted at the Zurich Open Repository and Archive, University of Zurich

ZORA URL: <https://doi.org/10.5167/uzh-24506>

Journal Article

Accepted Version

Originally published at:

Hornemann, Thorsten; Penno, A; Rütli, M F; Ernst, D; Kivrak-Pfiffner, Fatma; Rohrer, L; von Eckardstein, Arnold (2009). The SPTLC3 subunit of serine palmitoyltransferase generates short chain sphingoid bases. *Journal of Biological Chemistry*, 284(39):26322-26330.

DOI: <https://doi.org/10.1074/jbc.M109.023192>

THE SPTLC3 SUBUNIT OF SERINE- PALMITOYLTRANSFERASE GENERATES SHORT CHAIN SPHINGOID BASES

Thorsten Hornemann^{1*}, Anke Penno¹, Markus F. Rütli, Daniela Ernst, Fatma Kivrak-Pfiffner,
Lucia Rohrer, Arnold von Eckardstein¹

Institute for Clinical Chemistry, University Hospital Zurich, Rämistrasse 100, CH-8091 Zurich,
Switzerland

¹ Competence Center for Systems Physiology and Metabolic Diseases, Zurich

* Corresponding Author: Institute for Clinical Chemistry, University Hospital Zurich, Rämistrasse
100, 8091 Zurich, Tel.: +41 1 255 4719, Fax: +41 1 255 4590, thorsten.hornemann@usz.ch

Abstract:

The enzyme serine-palmitoyltransferase (SPT) catalyses the rate limiting step in the *de-novo* synthesis of sphingolipids. Previously the mammalian SPT was described as a heterodimer composed of two subunits - SPTLC1 and SPTLC2. Recently we identified a novel third SPT subunit (SPTLC3). SPTLC3 shows about 68% identity to SPTLC2 and also includes a PLP consensus motif. Here we report that the overexpression of SPTLC3 in HEK293 cells leads to the formation of two new sphingoid base metabolites, namely C₁₆-sphinganine and C₁₆-sphingosine. SPTLC3 expressing cells have higher *in-vitro* SPT activities with lauryl- and myristoyl-CoA than SPTLC2 expressing cells and SPTLC3 mRNA expression levels correlate closely with the C₁₆-sphinganine synthesis rates in various human and murine cell lines. Approximately 15% of the total sphingolipids in human plasma contain a C₁₆ backbone and are found in the high density- and low density- but not the very low density lipoprotein fraction. In conclusion we show that the SPTLC3 subunit is generating C₁₆- sphingoid bases and that sphingolipids with a C₁₆ backbone constitute a significant proportion of human plasma sphingolipids.

Introduction:

Sphingolipids comprise a class of bioactive lipids that contribute to plasma membrane and plasma lipoprotein formation and exert a broad range of cellular signaling functions, such as cell proliferation, endocytosis, and the response of cells to inflammatory and apoptotic stress signals (1-4).

Sphingolipids are derived from the aliphatic amino alcohol sphingosine which is formed from the precursors L-serine and palmitoyl-CoA. The condensation of serine with palmitoyl-CoA is catalyzed by the enzyme serine-palmitoyltransferase (SPT) [EC 2.3.1.50] and leads to the intermediate 3-ketodihydrosphingosine (3-KDS). 3-KDS is then rapidly converted to dihydrosphingosine (sphinganine) and dihydroceramide. The desaturation of dihydroceramide generates ceramide and the breakdown of ceramide by ceramidase finally forms sphingosine. The sphingosine backbone of ceramide is usually O-linked to a polar head group such as phosphocholine or carbohydrates and amide-linked to an acyl group. The combination of the sphingosine backbone with different head groups, in particular with various oligosaccharides, leads to a complex variety of different sphingolipid metabolites (5,6). Moreover, it was shown recently that SPT is also able to use L-

alanine as an alternative substrate thereby generating the atypical sphingoid base 1-deoxy-sphinganine (7).

SPT belongs to the family of pyridoxal phosphate (PLP)-dependent α -oxoamine synthases (POAS). Other members of this family include 5-amino-levulinic acid synthase, 2-amino-3 ketobutyrate ligase (KBL) and 8-amino-7-oxononanoate synthase (AONS) (8). SPT is ubiquitously expressed and enzyme activity has been detected in all tissues tested so far including brain, lung, liver, kidney and muscle (9). SPT is essential for embryonic development and homozygous SPT knockout mice are not viable (10). SPT has been believed to be a heterodimer composed of two subunits SPTLC1 and SPTLC2. The two subunits SPTLC1 and SPTLC2 show a similarity at AA level of ~20% and are highly conserved among species. Although both subunits seem to be required for enzyme activity only the SPTLC2 subunit contains a PLP binding motif (8,11).

Recently, we identified and cloned a novel, third SPT subunit (SPTLC3) (12). The SPTLC3 sequence shows 68% homology to the SPTLC2 subunit and also includes a PLP consensus motive. The SPTLC3 gene is present in mammals, birds and some lower vertebrates like fish (*D. rerio*) and frog (*X. laevis*) but not in invertebrate lineages. The SPTLC3 mRNA has been detected in most human tissues with a particularly high expression in placenta (12), indicating a special role for SPTLC3 during development and pregnancy. By using immunoprecipitation, native gel analysis, crosslinking studies and size exclusion chromatography it was demonstrated that the native SPT enzyme contains all three subunits and forms a protein complex with a molecular mass of about 460 kDa (13). However, since SPTLC2 and SPTLC3 are encoded by two distinct genes and expressed within the same cell types we assume a distinct function for the two subunits. One of these differences might be altered substrate

affinity or enzymatic activity. This issue is addressed in the present study.

Experimental procedures

Cell lines

HEK293 cells were obtained from ATCC and cultured in full medium (DMEM, Sigma) containing 10% fetal bovine serum (Fischer scientific) and Penicillin/Streptomycin (100 units per ml/0.1mg per ml).

HEK293 cells were transfected with lipofectamine 2000 (Invitrogen) and selected for neomycine resistance (G418, 400 μ g/ml) to generate a pool of stably expressing cells. The expression of each of the SPT subunits in the three cell lines was confirmed by western blots.

Fumonisin B1 dependent accumulation of sphingoid bases

Fumonisin B1 (Sigma) was added to the media of exponentially growing cells at a final concentration of 10 μ g/ml. As a negative control myriocin (10 μ g/ml, Sigma) was added together with Fumonisin B1. 24h after Fumonisin B1 addition, cells were washed twice with PBS, harvested and counted (coulter® Z2, Beckman Coulter). Synthetic C17 sphingosine (Avanti Polar Lipids) was added to each sample as an internal extraction standard.

SPT activity assay

Cells were grown in 10 cm dishes to approximately 80% confluency. Medium was removed and the cells were washed two times with PBS and harvested in 1ml of PBS by scraping. The suspension was transferred into a 1.5 ml reaction tube. Cells were pelleted by centrifugation (2500 g, 2 min at 4°C) and resolved in assay buffer (50 mM Hepes pH 8.0, 0.5 mM MnCl₂). The protein concentration was adjusted to 2 mg/ml. Protein concentrations of the cell lysates were determined using the Bradford Assay (Bio-Rad). Albumin was used as calibration standard.

The reaction cocktail for measuring *in-vitro* SPT activity was composed of 400 μ g total lysate protein, 50 mM Hepes (pH

8.0), 0.5 mM L-serine, 0.05 mM palmitoyl-CoA, 20 μ M pyridoxal-5'-phosphate, 0.5 mM MnCl_2 , 0.1 μCi L-[U- ^{14}C]serine (Amersham) in a total volume of 200 μl . The assay was performed at 37°C for 60 min. For the negative controls SPT activity was specifically blocked by the addition of the SPT inhibitor myriocin (40 μM , Sigma). The reaction was stopped by adding 0.5 ml methanolic-KOH: CHCl_3 (4:1) to the mixture. Methanolic KOH was prepared by dissolving 0.7 g KOH pellets in 100 ml MeOH. Lipids were extracted at 37°C under steady agitation for 30 min. Subsequently 500 μl CHCl_3 , 500 μl alkaline water (100 μl NH_4 (2 N) in 100 ml H_2O) and 100 μl NH_4 (2 N) was added in this order. Phases were separated by centrifugation (13000 g, 5 min) and the upper phase discarded. The lower phase was washed three times with alkaline water. Finally the lower organic phase was transferred to a scintillation vial and the CHCl_3 evaporated under a stream of N_2 . After the addition of scintillation cocktail the radioactivity was quantified on a Scintillation Analyzer (Packard Liquid 1900TR).

Quantitative RT-PCR

The mRNA was extracted using Tri Reagent (Molecular Research Center, Inc., Cincinnati, US) and transcribed to cDNA using oligo dT primers and Superscript III (Invitrogen) according to manufacturer's instructions. Specific primers for the different SPT subunits were designed using the Oligo6.0 software (Molecular Biology Insights, Cascade, USA). Light Cycler PCR was performed using the DNA Master Kit (Roche Diagnostics, Rotkreuz, Switzerland) according to the manufacturer's instructions. The following primer pairs were used (0.4 μM each):

huSPTLC3fw: 5'-
TGCAGCCAAGTATGATGAGTCTA-3';
huSPTLC3rv: 5'-
GCAGATGCACGATGGAAC-3'
moSPTLC3fw: 5'-
GGCTTGCAGGGAAATATG-3';
huSPTLC3rv: 5'-
GGATGACTGAAGTGTGGTTA-3'

Amplification was carried out for SPTLC3: 50 cycles, each consisting of 10 s at 95 °C; 10 s at 61°C; 20 s at 72°C. The linearity of the assays was determined by serial dilutions of the templates for each primer set separately.

Separation of plasma lipoproteins

Plasma was isolated from healthy normolipidemic donors after overnight fasting. Three ml plasma was fractionated on a four step density gradient essentially as described (14). Ultracentrifugation was performed in a Beckman SW-40 swinging bucket rotor for 24 h at 41000 rpm at 15°C. Fractions (1 ml) were collected from the top of the centrifuge tube and analyzed for triglyceride, cholesterol and other lipids.

Lipid extraction and hydrolysis

Total lipids were extracted and, prior to analysis, either base or acid/ base hydrolyzed (15). Briefly, cells were resuspended in 200 μl PBS and lipids extracted in 1 ml extraction buffer (2 vol. methanol/1 vol. chloroform + 0.15 $\mu\text{l/ml}$ C17 SO (1mM in EtOH). 100 μl of NH_4 (2 N) was added and the lipids were extracted under constant agitation (1 h, 37°C). Subsequently 0.5 ml chloroform was added and samples were centrifuged (12000 g, 5 min) to separate the organic from the water phase. The upper (water) phase was discarded and the lower phase washed twice with 1 ml of alkaline water (1 ml NH_4 (2 N) in 100 ml water) and dried under N_2 . For acid hydrolysis, the dried lipids were resuspended in 200 μl methanolic HCl (1 N HCl/10 M water in methanol) and kept at 65°C for 12-15 hours. The solution was neutralized by the addition of 40 μl KOH (5 M) and subsequently subjected to as follows: 0.5 ml extraction buffer (4 vol. 0.125 M KOH in methanol + 1 vol. chloroform) was added and mixed. Subsequently, 0.5 ml chloroform, 0.5 ml alkaline water and 100 μl NH_4 (2 N) was added in this order. Liquid phases were separated by centrifugation (12000 g, 5 min). The upper phase was aspirated and the lower phase washed twice with alkaline water. Finally, the lipids were dried by evaporation of the

chloroform phase under N₂ and subjected to LC-MS analysis.

Plasma lipids were analyzed from 100 µl of human EDTA-treated plasma which was treated in the same manner.

LC-MS

Extracted lipids were solubilized in 56.7% methanol/33.3% ethanol/10% water and derivatized with ortho-phthaldialdehyde (OPA, Sigma) (15). The lipids were separated on a C₁₈ column (Uptisphere 120Å, 5µm, 125x2mm, Interchim, France) and analyzed by a serial arrangement of a fluorescence detector (HP1046A, Hewlett Packard) followed by a MS detector (LCMS-2010A, Shimadzu). APCI (atmospheric pressure chemical ionisation) was used for ionisation. Non natural C₁₇ sphingosine (Avanti Polar Lipids) was used as the internal standard.

Results

SPTLC3 expressing cells generate C₁₆ sphingoid bases

The human SPT subunits SPTLC1, SPTLC2 and SPTLC3 were cloned into a pcDNA3.1 expression vector and expressed in HEK293 cells as reported earlier (12). HEK293 cells were chosen since they express low endogenous levels of SPTLC3 mRNA (Fig.4A). All subunits were expressed at comparable levels as demonstrated by western blot analysis and showed no signs of degradation (12).

To determine if SPTLC3 expressing cells generated more, or other, sphingoid bases we compared the spectrum of *de novo*-synthesized sphingoid bases between SPTLC3 deficient (HEK^{Cnt}) and SPTLC3 overexpressing cells (HEK^{SPTLC3}). This was done by blocking the *de novo* synthesis pathway at the step of the ceramide synthase (CerS) with Fumonisin B1 (FB1). The inhibition of CerS leads to a time dependent accumulation of its substrate sphinganine (SA). Hence, potential side products of the SPT reaction are also accumulating under these conditions (7). The accumulated lipids were extracted 24h after the addition of FB1, derivatized with ortho-

phthaldialdehyde (OPA) and analyzed on a C₁₈ reverse phase column with a serially arranged fluorescence and MS detector (15).

In the presence of FB1 we observed a significant accumulation of sphinganine (Fig.1A) whereas no SA accumulation was seen when SPT activity was blocked with myriocin. In parallel we observed the appearance of a second unknown peak which eluted prior to SA after 8.2 min. Because of similar retention times this peak was partly overlaid by the internal standard (C₁₇-SO) which was added for normalization. (Fig.1B). Accumulation of SA but also of this unknown peak was not observed when SPT activity was inhibited with myriocin. This observation indicates that the unknown metabolite is a product of the SPT reaction. Subsequent MS analysis revealed that the unidentified metabolite had an m/z of 450.3 (as an OPA derivate). For this mass the single ion chromatogram revealed a single peak with the same retention time as seen in the fluorescence chromatogram (Fig.1B). This signal was not seen in the presence of myriocin (Fig. 1C). The unknown metabolite (m/z 450.3) showed a mass difference to sphinganine (m/z 478.3) of 28 Da which equals the mass of a CH₂CH₂ group and suggests that the unknown metabolite is dihydro-sphingosine (SA) with a C₁₆, instead of a C₁₈, carbon chain (C₁₆-SA). This metabolite could be formed by the conjugation of L-serine with myristoyl-CoA instead of palmitoyl-CoA.

SPTLC3 has higher activity with C₁₂ and C₁₄ acyl-CoA

To test this hypothesis we compared the *in-vitro* SPT activity with various acyl-CoA substrates in extracts from control, SPTLC1-, SPTLC2- and SPTLC3-overexpressing cells. All acyl-CoAs were used at the same concentration (50 µM). In comparison the SPTLC3 expressing cells showed a significantly higher activity with lauryl-CoA and myristoyl-CoA than did the control, SPTLC1- or SPTLC2-expressing cells (Fig.2A). This suggests

that the SPTLC3-mediated SPT activity is primarily responsible for the generation of sphingoid bases with a C₁₄ or C₁₆ backbone whereas the SPTLC2 subunit seems to be more specific for longer acyl-CoAs thereby forming C₁₈ and C₂₀-sphingoid bases.

C₁₆-SA generation is stimulated by serine

The addition of L-serine to the cell culture medium generally stimulates SPT activity and SA *de-novo* synthesis (7). To determine if L-serine also stimulated SPTLC3 mediated C₁₆-SA generation, we compared the accumulation of C₁₆-SA in FB1 treated HEK^{Cnt} and HEK^{SPTLC3} cells which were cultured either in regular medium or in medium that was supplemented with L-serine (10 mM). The normally cultured HEK^{SPTLC3} cells showed a clear accumulation of C₁₆-SA in the presence of FB1, whereas HEK^{Cnt} cells did not show any accumulation under these conditions (Fig. 2B). In the cells which were cultured at elevated serine levels the accumulated sphingoid bases increased significantly. For HEK^{SPTLC3} cells we observed a 3-fold increase in SA accumulation (data not shown) and a 4-fold increase in the accumulation of C₁₆-SA (Fig. 2B). Even in HEK^{Cnt} cells a small accumulation of C₁₆-SA was detected under these conditions.

Kinetic analysis of SPTLC3 activity

To obtain further insight into the enzymatic mechanism we compared the kinetics for myristoyl-CoA and palmitoyl-CoA in HEK^{Cnt} and HEK^{SPTLC3} cells. For palmitoyl-CoA the enzyme followed a Michaelis-Menten kinetics up to a concentration of about 0.1 mM (Fig. 3A). The kinetics with palmitoyl-CoA was essentially the same in HEK^{Cnt} and HEK^{SPTLC3} cells. At palmitoyl-CoA concentrations above 0.15 mM substrate inhibition was observed in accordance to earlier reports (16,17). Also the Hanes-Woolf plot (18) showed a linear relationship between [S] and 1/v up to a palmitoyl-CoA concentration of 0.1mM (Fig. 3A). For myristoyl-CoA we observed

an about 5-fold higher activity in HEK^{SPTLC3} cells compared to HEK^{Cnt} cells (Fig. 3B). As for palmitoyl-CoA we also observed an inhibitory effect of myristoyl-CoA at higher concentrations. For both substrates the optimal activity was in a concentration range of 0.1-0.125 mM.

K_m and V_{max} values (Fig. 3C) were deduced from the Hanes-Woolf plots and confirmed by a hyperbolic regression analysis (19). Both methods gave similar results.

For palmitoyl-CoA the kinetic parameters V_{max} and K_m were similar in HEK^{Cnt} and HEK^{SPTLC3} cells whereas for myristoyl-CoA both cell lines showed significant differences. Due to the low activity in HEK^{Cnt} cells a precise determination of V_{max} and K_m for myristoyl-CoA was not possible. Nevertheless, it was obvious that the V_{max} for myristoyl-CoA is significantly lower in HEK^{Cnt} compared to HEK^{SPTLC3} cells. The K_ms for palmitoyl-CoA and myristoyl-CoA in HEK^{SPTLC3} cells were comparable whereas the maximal velocity for myristoyl-CoA was about 50% lower than for palmitoyl-CoA (Fig. 3C).

SPTLC3 mRNA levels correlate with C₁₆-SA accumulation in FB1 blocked cells

To further confirm that the generation of C₁₆-SA is linked to the expression of SPTLC3, we analysed the SPTLC3 mRNA levels in various human and non-human cell lines (Fig.4A). Some cell lines like HEK293 or the human monocytic cell line THP1, showed very low SPTLC3 mRNA expression whereas intermediate levels were found in HepG2, COS and NIH/3T3 cells. The highest SPTLC3 mRNA levels were in the trophoblast lines JAR and JEG-3 as reported earlier (12). The SPTLC3 mRNA levels showed a close correlation with the levels of accumulated C₁₆-SA in these cells (Fig. 3B), providing further evidence that C₁₆-sphingoid bases are primarily generated by SPTLC3.

C₁₆-SA is metabolized to C₁₆-SO

The observation that C₁₆-SA accumulates in the presence of the CerS inhibitor FB1 indicates that C₁₆-SA is also a substrate for CerS. Consequently, the generated C₁₆-SA is further metabolized to C₁₆-dihydro-ceramide and to C₁₆-ceramide. The degradation of C₁₆-ceramide by ceramidase would finally lead to the generation of C₁₆-sphingosine (C₁₆-SO).

To test whether the SPTLC3-expressing cells also produce C₁₆-SO we compared the total sphingoid base content between HEK^{Cnt} and HEK^{SPTLC3} cells. In view of the great variety of fatty acids and possible head groups that can be attached to the sphingoid backbone, a complete analysis of all possible C₁₆-ceramide variants is a demanding task and will be addressed in future studies. To simplify the analysis we, therefore, subjected the extracted lipids to acid and base hydrolysis. Under acidic conditions the amide bond of the conjugated fatty acid is released whereas the O-linked phosphoester and carbohydrate moieties of the sphingoid base head group are removed under basic conditions. This procedure allowed the quantification of the total C₁₆ and C₁₈ sphingoid base levels in the cells. The molecular mass of SO and SA differs, due to the Δ⁴ double bond, by two Daltons. As described above we observed a significant FB1 dependent accumulation of C₁₆-SA (m/z 450.3) in HEK^{SPTLC3} cells (Fig. 5A). No signal in the single mass chromatogram for C₁₆-SO (m/z 448.3) was seen because the metabolism of the de-novo formed C₁₆-SA was blocked in the presence of FB1. In contrast, analysis of the acid/base treated extract from HEK^{SPTLC3} cells showed a pronounced peak with the m/z ratio of C₁₆-SO (448.3). Interestingly, HEK^{Cnt} cells also contained small but detectable amounts of C₁₆-SO but did not show the accumulation of C₁₆-SA in the presence of FB1. This could be possibly explained by an uptake of C₁₆-ceramide from the medium as an external source since mammalian serum, including fetal calf serum (FCS) contains considerable

amounts of C₁₆-based sphingolipids (see also Fig. 6).

To further demonstrate that the identified metabolite is C₁₆-SO we compared its retention time with respect to other sphingoid bases with different carbon chains. On a C₁₈ reverse phase column sphingoid bases show a logarithmic correlation between retention time and their carbon chain length (Fig. 5B). Regression analysis of this function revealed a theoretical retention time for C₁₆-SO of 6.5 min which is in agreement with the observed retention time (6.45 min) of the identified metabolite (Fig. 3A,B).

Our studies also show that the C₁₆-SO levels of acid/base treated cell lines closely correlate with C₁₆-SA which can be assumed to be the metabolic precursor (Fig. 5C).

Up to 15% of human plasma sphingolipids are based on a C₁₆-backbone

The observation that SPTLC3 is responsible for the generation of C₁₆-sphingoid bases raised the questions of whether these lipids are also present in human plasma and how they are transported in plasma.

We analyzed plasma samples of 20 healthy donors. The plasma was acid/base treated and analyzed by LC-MS. The analysis showed that the majority of plasma sphingolipids are based on a C₁₈ sphingosine backbone. Nevertheless, an astonishingly high fraction of plasma sphingolipids was found with a C₁₆-SO backbone (Fig. 6A). The proportion of C₁₆-SO in total plasma SO may be as high as 15%. The fraction of plasma sphingolipids which contained a SA backbone was much lower. About 4% of the plasma sphingolipids contained a sphingosine backbone whereas 15-20% of the total SA contained a C₁₆-backbone.

The analysis of lipoprotein fractions which were isolated by ultracentrifugation demonstrated that both, the C₁₆- and the C₁₈-sphingolipids are present in the LDL and HDL fractions but not in the VLDL fraction (Fig. 6B). In comparison to total

cholesterol and triglyceride the sphingolipids showed a shoulder in fractions 9 and 10 indicating that they are also part of a denser HDL subfraction.

Discussion

The fact that SPTLC2 and SPTLC3 both form a catalytically active SPT holoenzyme raises questions about the functional differences between these two isoforms. Here we report that the presence of SPTLC3 enables the enzyme to metabolize shorter acyl-CoAs, like lauroyl- and myristoyl-CoA in contrast to the predominant usage of palmitoyl-CoA by SPT in the absence of SPTLC3. In HEK293 cells, which endogenously express insignificant levels of this subunit only, we observed the appearance of two novel sphingolipid metabolites in cells overexpressing SPTLC3. The two novel metabolites were identified as C₁₆-SA and C₁₆-SO. SPTLC3 expressing cells showed a significantly higher *in-vitro* SPT activity with lauroyl – and myristoyl-CoA compared to SPTLC1- or SPTLC2-overexpressing cells. The presence of these metabolites correlated closely with SPTLC3 mRNA expression in various human and murine cell lines. A kinetic comparison between HEK^{Cnt} and HEK^{SPTLC3} cells showed a significantly higher V_{max} for myristoyl-CoA in the SPTLC3 expressing cells whereas V_{max} for palmitoyl-CoA was the same in both cell lines. This observation suggests that the reaction with palmitoyl-CoA is primarily catalyzed by the (endogenously expressed) SPTLC2 subunit and is not influenced by the presence of SPTLC3. Quantitative RT-PCR analysis of HEK^{Cnt} and HEK^{SPTLC3} cells showed that SPTLC1 and SPTLC2 mRNA levels do not change upon SPTLC3 expression (data not shown), implying that the SPTLC3 subunit has a rather specific affinity for myristoyl-CoA and only a minor affinity for palmitoyl-CoA. Otherwise the overexpression of SPTLC3 would have influenced the V_{max} for palmitoyl-CoA as well. These findings suggest that SPTLC3

is predominantly responsible for the generation of C₁₄ and C₁₆-sphingoid bases, making SPTLC3 functionally distinct from the SPTLC2 subunit. Previously, Merrill and co-workers analyzed SPT activities with different fatty acid-CoA thioesters in microsomes of various rat tissues (9). Some of the tested tissues showed higher activities with shorter alkyl chains than others. This observation might be explained by different SPTLC3 expression levels in these tissues.

The identification of three SPT subunits two of which contain a binding site for the PLP cofactor, raises further questions about the structure of the SPT holoenzyme. In analogy to other members of the POAS family it has been assumed that the active SPT is a heterodimer. However, size exclusion chromatography and cross-linking data indicate that the SPT is a holoenzyme and simultaneously composed of all three subunits (13). It is not clear yet whether all three subunits are required to form an active SPT enzyme. The fact that some cells, like HEK293, express only minor levels of this subunit indicate that SPTLC3 is not essential for forming an active enzyme. Nevertheless, the size exclusion chromatography data revealed a molecular mass of 460 kDa for the active SPT complex – independent of the presence or absence of SPTLC3 (13). This might be explained by a dynamic stoichiometry of the complex in which the SPTLC2 and SPTLC3 subunits can substitute for each other. A second possibility would be an association with further yet unidentified proteins. In this context it is interesting that, very recently, a fourth SPT subunit was reported (20). Han et al. identified two short polypeptides which interact with SPTLC1 and SPTLC2. The expression of these two proteins stimulated SPT activity and modulated the substrate preference of SPT towards the use of longer acyl-CoA (20), indicating a regulatory function for these polypeptides. However, it is currently not clear how these new proteins can be integrated into the concept of SPT structure and function.

Besides C₁₆-SA, we also observed the presence of C₁₆-SO in acid/base treated lipid extracts of SPTLC3-expressing cells. Since a C₁₆-SO standard is commercially not available the identification of this metabolite is based on several indirect pieces of evidence. The conformity of the identified C₁₆-SO is based on its mass (Fig. 5A), the retention time (Fig. 5B) and the correlation with its precursor C₁₆-SA (Fig. 5C). We also confirmed the presence of this metabolite in lipid extracts from *Drosophila* (data not shown); insects have been reported to generate primarily C₁₆-sphingoid bases (21). Thus, it appears that C₁₆-SA can be further metabolized to C₁₆-dihydro-ceramide/C₁₆-ceramide and finally also degraded to C₁₆-SO. This indicates that potentially all types of sphingolipids, including glyco- and phosphosphingolipid, could be formed on the basis of a C₁₆ sphingosine backbone. These findings greatly expand the already huge variety of possible sphingolipid variants and might also influence the understanding of these lipids. In comparison to C₁₈ sphingoid bases sphingoid bases with a C₁₆ backbone are considerably less hydrophobic and hence likely exhibit significant differences in biophysical properties. The C₁₆ - sphingolipids will exchange much more rapidly with a hydrophilic environment which might influence their subcellular localization and their distribution in membranes which, in turn, may have important implications for transport and translocation as well as cellular signal transduction.

Curiously there are only few reports on C₁₆-sphingolipids in the literature. Sphingoid bases with a C₁₄ and C₁₆ carbon chain are the predominant sphingolipids in insects (21,22). Recent studies of a marine virus (Coccolithovirus) revealed that the viral genome contains a cluster of putative sphingolipid biosynthetic genes, including an SPT-like enzyme (23) that utilizes myristoyl-CoA and therefore generates C₁₆ sphingoid bases when expressed in yeast. Sphingoid bases with 16 carbon atoms were also found in bovine milk (24,25) and

as a part of the black epidermis from the antarctic minke whale (26). A few earlier reports indicate the presence of C₁₆ sphingoid bases in human plasma (27,28). Interestingly, certain human tissues like placenta show pronounced expression of SPTLC3 (12) and contain high levels of C₁₆ sphingoid bases (data not shown). This was also seen in human trophoblast cell lines like JEG-3 and JAR in which high SPTLC3 mRNA expression correlated with high C₁₆ sphingoid base levels (Fig. 4B). The unusually high level of SPTLC3 mRNA in placental tissue suggests a specific physiological role for these metabolites during embryogenesis and pregnancy. Also, the finding that approximately 15% of human plasma sphingolipids contain a C₁₆ backbone indicates a significant physiological relevance of these metabolites. The source of the C₁₆ sphingolipids in plasma is not yet known but we have demonstrated that plasma C₁₆- and C₁₈-sphingoid bases are transported in HDL and LDL but not in the VLDL lipoproteins fraction (Fig. 6B) indicating that C₁₆-sphingoid bases are at least partly metabolized by the liver. In this respect it is interesting that elevated plasma sphingolipid levels are associated with an increased risk of developing atherosclerosis and coronary heart disease (29,30). Myriocin lowered plasma sphingolipids in ApoE knock-out mice and significantly reduced the formation of atherosclerotic lesions in these mice and showed a significant delay of disease progression (31-33). Since treatment with myriocin would be expected to lower the levels of both C₁₆- and C₁₈-based sphingolipids it would be interesting to determine if one of the two subclasses is primarily involved in the pathogenesis of atherosclerosis. In this context, analysis of the C₁₆-sphingoid bases in plasma of 15 wild-type mice (C57BL/6) showed significantly lower levels (about 90% less) of C₁₆ sphingoid bases in mice although the levels of the C₁₈ sphingoid bases were comparable (data not shown). Low levels of C₁₆-sphingoid bases were also seen in

rat plasma (data not shown). On the other hand, rodent and human cell lines showed similar SPTLC3 activities when normalized to mRNA expression (Fig. 4B), indicating that the lower C₁₆-SO levels in mouse plasma are due to a different C₁₆-SO metabolism and not simply caused by a lower SPTLC3 activity in mice. It should therefore be considered that rodents and humans are distinct with respect to C₁₆-sphingolipid metabolism, a fact that should

be kept in mind when working with rodent models of disease. In conclusion, the observation that SPTLC3 is found in all higher vertebrates and that its presence is primarily linked to the generation of C₁₆ sphingoid bases, indicate an evolutionarily conserved need for these types of sphingolipids. However, the distribution, metabolic fate and biochemical properties of these lipids have to be addressed in future studies.

Acknowledgments:

We would like to thank Yu Wei for her assistance during this project as well as Michael Fitzgerald for his helpful comments and suggestions and especially Jean Vance for having a final look at the manuscript.

We also thank the Foundation for scientific research (Forschungskommission, University of Zurich), the Hartmann Müller Foundation, the German Society for Clinical Chemistry and Laboratory Medicine (DGKL), the EMDO Foundation and the European Commission (LSHM-CT-2006-037631) for financially supporting this work.

References:

1. Hannun, Y. A., and Obeid, L. M. (2008) *Nat Rev Mol Cell Biol* **9**, 139-150
2. Wymann, M. P., and Schneider, R. (2008) *Nat Rev Mol Cell Biol* **9**, 162-176
3. Saddoughi, S. A., Song, P., and Ogretmen, B. (2008) *Subcell Biochem* **49**, 413-440
4. Zheng, W., Kollmeyer, J., Symolon, H., Momin, A., Munter, E., Wang, E., Kelly, S., Allegood, J. C., Liu, Y., Peng, Q., Ramaraju, H., Sullards, M. C., Cabot, M., and Merrill, A. H., Jr. (2006) *Biochim Biophys Acta* **1758**, 1864-1884
5. Pruett, S. T., Bushnev, A., Hagedorn, K., Adiga, M., Haynes, C. A., Sullards, M. C., Liotta, D. C., and Merrill, A. H., Jr. (2008) *J Lipid Res*
6. Merrill, A. H., Jr. (2005) *Glycobiology* **15**, 15G
7. Zitomer, N. C., Mitchell, T., Voss, K. A., Bondy, G. S., Pruett, S. T., Garnier-Amblard, E. C., Liebeskind, L. S., Park, H., Wang, E., Sullards, M. C., Merrill, A. H., Jr., and Riley, R. T. (2008) *J Biol Chem*
8. Hanada, K. (2003) *Biochim Biophys Acta* **1632**, 16-30
9. Merrill, A. H., Jr., Nixon, D. W., and Williams, R. D. (1985) *J Lipid Res* **26**, 617-622
10. Hojjati, M. R., Li, Z., and Jiang, X. C. (2005) *Biochim Biophys Acta* **1737**, 44-51
11. Hanada, K., Hara, T., Nishijima, M., Kuge, O., Dickson, R. C., and Nagiec, M. M. (1997) *J Biol Chem* **272**, 32108-32114
12. Hornemann, T., Richard, S., Rutti, M. F., Wei, Y., and von Eckardstein, A. (2006) *J Biol Chem* **281**, 37275-37281
13. Hornemann, T., Wei, Y., and von Eckardstein, A. (2007) *Biochem J* **405**, 157-164
14. Kelley, J. L., and Kruski, A. W. (1986) *Methods Enzymol* **128**, 170-181
15. Riley, R. T., Norred, W. P., Wang, E., and Merrill, A. H. (1999) *Nat Toxins* **7**, 407-414
16. Merrill, A. H., Jr., and Williams, R. D. (1984) *J Lipid Res* **25**, 185-188
17. Williams, R. D., Wang, E., and Merrill, A. H., Jr. (1984) *Arch Biochem Biophys* **228**, 282-291
18. Wong, J. T., and Hanes, C. S. (1962) *Can J Biochem Physiol* **40**, 763-804
19. Duggleby, R. G. (1981) *Anal Biochem* **110**, 9-18
20. Han, G., Gupta, S. D., Gable, K., Niranjanakumari, S., Moitra, P., Eichler, F., Brown, R. H., Jr., Harmon, J. M., and Dunn, T. M. (2009) *Proc Natl Acad Sci U S A*
21. Fyrst, H., Herr, D. R., Harris, G. L., and Saba, J. D. (2004) *J Lipid Res* **45**, 54-62
22. Fyrst, H., Zhang, X., Herr, D. R., Byun, H. S., Bittman, R., Phan, V. H., Harris, G. L., and Saba, J. D. (2008) *J Lipid Res* **49**, 597-606
23. Han, G., Gable, K., Yan, L., Allen, M. J., Wilson, W. H., Moitra, P., Harmon, J. M., and Dunn, T. M. (2006) *J Biol Chem* **281**, 39935-39942
24. Byrdwell, W. C., and Perry, R. H. (2007) *J Chromatogr A* **1146**, 164-185
25. Karlsson, A. A., Michelsen, P., and Odham, G. (1998) *J Mass Spectrom* **33**, 1192-1198
26. Yunoki, K., Ishikawa, H., Fukui, Y., and Ohnishi, M. (2008) *Lipids* **43**, 151-159
27. Katsikas, H., and Wolf, C. (1995) *Biochim Biophys Acta* **1258**, 95-100
28. Samuelsson, B., and Samuelsson, L. (1969) *J Lipid Res* **10**, 47-55
29. Jiang, X. C., Paultre, F., Pearson, T. A., Reed, R. G., Francis, C. K., Lin, M., Berglund, L., and Tall, A. R. (2000) *Arterioscler Thromb Vasc Biol* **20**, 2614-2618
30. Schissel, S. L., Tweedie-Hardman, J., Rapp, J. H., Graham, G., Williams, K. J., and Tabas, I. (1996) *J Clin Invest* **98**, 1455-1464
31. Park, T. S., Panek, R. L., Mueller, S. B., Hanselman, J. C., Rosebury, W. S., Robertson, A. W., Kindt, E. K., Homan, R., Karathanasis, S. K., and Rekhter, M. D. (2004) *Circulation* **110**, 3465-3471

32. Park, T. S., Panek, R. L., Rekhter, M. D., Mueller, S. B., Rosebury, W. S., Robertson, A., Hanselman, J. C., Kindt, E., Homan, R., and Karathanasis, S. K. (2006) *Atherosclerosis* **189**, 264-272
33. Hojjati, M. R., Li, Z., Zhou, H., Tang, S., Huan, C., Ooi, E., Lu, S., and Jiang, X. C. (2005) *J Biol Chem* **280**, 10284-10289

Figure legends

Figure 1: A) HPLC analysis of accumulated lipids in FB1-treated HEK^{SPTLC3} cells. HEK^{SPTLC3} cells were cultured in the presence of Fumonisin B1 (FB1) for 24 h. The accumulated sphingoid bases were extracted, derivatized with ortho-phthaldialdehyde (OPA) and analyzed on a C18 reverse phase column with fluorescence detection. In the presence of FB1 (black line) sphinganine accumulated (SA, RT 13.5min) and a second unknown metabolite appeared (RT 8.2 min). This unknown metabolite was partially superimposed by the internal standard (C17-SO) due to the similar retention times. No accumulation of these metabolites was observed when the cells were treated with the SPT inhibitor myriocin (grey line). B) MS analysis with a serially arranged MS detector revealed an m/z of 450.3 for the unknown metabolite. The single ion chromatogram showed a single peak (m/z 450.3, grey line) with a retention time identical to that observed in the fluorescence spectrum. The internal standard (C17-SO, m/z 462.3, thin black line) eluted shortly before the unknown metabolite. C) SA and the unknown metabolite did not accumulate in FB1+myriocin-treated HEK^{SPTLC3} cells.

Figure 2: A) *In vitro* SPT activity with various acyl-CoA substrates in control, SPTLC1, SPTLC2 and SPTLC3 overexpressing HEK293 cells. SPTLC3 overexpressing cells showed a significantly higher activity with lauroyl (C₁₂) - and myristoyl (C₁₄) -CoA compared to cells expressing the empty vector or the subunits SPTLC1 or SPTLC2. The activity with stearoyl and oleoyl-CoA was comparable for all cell lines. (For comparison the activity with palmitoyl-CoA is defined as 100%). B) Effect of serine supplementation on C₁₆-SA generation in cultured HEK^{Cnt} and HEK^{SPTLC3} cells. Cells were treated with FB1 (24 h) and the accumulated C₁₆-SA quantified by LC-MS. A significant buildup of C₁₆-SA was seen in SPTLC3-expressing cell but not in control cells. The addition of L-serine (10 mM) to the cell culture medium of SPTLC3 cells increased the generation of C₁₆-SA ~ 4-fold.

Figure 3: Kinetic analysis of SPTLC3 activity in HEK^{Cnt} and HEK^{SPTLC3} for palmitoyl-CoA and myristoyl-CoA. A) For palmitoyl-CoA both cell lines show an identical kinetic behavior. The kinetics followed a Michaelis-Menten curve up to a substrate concentration of 0.1 mM (left panel). Above that concentration activity was reduced due to substrate inhibition. The Hanes-Woolf representation (right panel) revealed an inverse linear correlation between substrate concentration and reaction velocity. B) HEK^{SPTLC3} cells showed significantly increased activity with myristoyl-CoA in comparison to control cells (HEK^{Cnt}). Also with myristoyl-CoA we observed a Michaelis-Menten kinetic up to 0.1mM and substrate inhibition at higher concentrations. Maximal activity was seen at myristoyl-CoA concentrations between 0.1-0.125mM. The Hanes-Woolf plot for myristoyl-CoA also showed an inverse linear correlation between substrate concentration and reaction velocity. C) V_{max} and K_m values were deduced from the Hanes blot and confirmed by a hyperbolic regression analysis. With palmitoyl-CoA the V_{max} and K_m values were identical for both cell lines whereas V_{max} for myristoyl-CoA was significantly lower in control cells (HEK^{Cnt}) compared to the SPTLC3-expressing cells (HEK^{SPTLC3}). In HEK^{SPTLC3} cells, the K_m for myristoyl-CoA and palmitoyl-CoA were comparable whereas V_{max} for myristoyl-CoA was about 50% lower than for palmitoyl-CoA. For HEK^{Cnt} cells the K_m and V_{max} of myristoyl-CoA could not be reliably determined (n.d.) due to low enzymatic activity with myristoyl-CoA in these cells.

Figure 4: A) Quantitative analysis of SPTLC3 mRNA expression in human and non-human cell lines. Cell lines like HEK293, THP1 or Hela express SPTLC3 in low amounts whereas higher expression was observed in the trophoblast cell lines JAR and Jeg3. B) Correlation of SPTLC3 mRNA expression and the accumulated C₁₆-SA in FB1-treated cells. Cells were

incubated with FB1 for 24h and the accumulated C₁₆-SA analyzed by LS-MS. We found a good correlation between SPTLC3 mRNA expression levels and the levels of accumulated C₁₆-SA ($R^2 = 0.98$).

Figure 5: A) Identification of C₁₆-SO in total lipid extract of HEK^{SPTLC3} cells. The diagram shows the single ion chromatograms for C₁₆-SA (450.3) and C₁₆-SO (448.3) in FB1 blocked and acid/base treated lipid extracts from HEK^{Cnt} and HEK^{SPTLC3} cells. The FB1 treated HEK^{SPTLC3} cells showed a significant accumulation of C₁₆-SA (450.3) which was not seen in the HEK^{Cnt} cells. No C₁₆-SA was observed in the acid/base treated lipid extracts from HEK^{SPTLC3} or HEK^{Cnt} cells. In its place a conspicuous peak appeared with the mass of C₁₆-SO (m/z 448.3) and a retention time of 6.5 min. This peak was significantly higher in HEK^{SPTLC3} than in HEK^{Cnt} cells. B) Functional relationship between retention time and carbon chain length of sphingoid bases. SA and SO standards with various carbon chain lengths were separated by HPLC. The dihydro-form (SA) generally eluted later than the corresponding SO form. The retention times showed a logarithmic relationship to the carbon chain length of the sphingoid bases. Based on a logarithmic regression analysis, a theoretical retention time of 6.45 min was calculated for C₁₆-SO which is in close concordance with the observed retention time for the C₁₆-SO peak (6.5 min). C) C₁₆-SA and C₁₆-SO levels in acid/base treated lipid extracts from various human and murine cell lines. The C₁₆-SO levels showed a good correlation to the precursor C₁₆-SA ($R^2 = 0.908$).

Figure 6: a) C₁₈- and C₁₆-SO levels in human plasma. Plasma of 20 healthy donors was acid/base treated and analyzed by LC-MS. The analysis revealed that the majority of plasma sphingolipids are based on a SO backbone whereas about 4% of the plasma sphingolipids contain a SA backbone. Up to 15% of the plasma sphingosine and sphinganine fraction was based on a C₁₆-backbone. B) C₁₈- and C₁₆-SO are components of plasma LDL and HDL-lipoprotein fractions. Human plasma was fractionated by a four step density gradient ultracentrifugation. The individual fractions were assayed for cholesterol (Chol; dotted line), triglycerides (TG; dashed line), C₁₈-SO (rhombus) and C₁₆-SO (square). The cholesterol and TG profile indicated the peak for LDL in fraction 4 and for HDL in fractions 7 and 8. In parallel the highest C₁₈-SO and C₁₆-SO concentrations were found in these fractions. The elevated TG concentrations in fraction 1 indicated the presence of VLDL which did not contain C₁₈-SO or C₁₆-SO. The sum of all fractions was defined as 100% and values are given in percent of total.

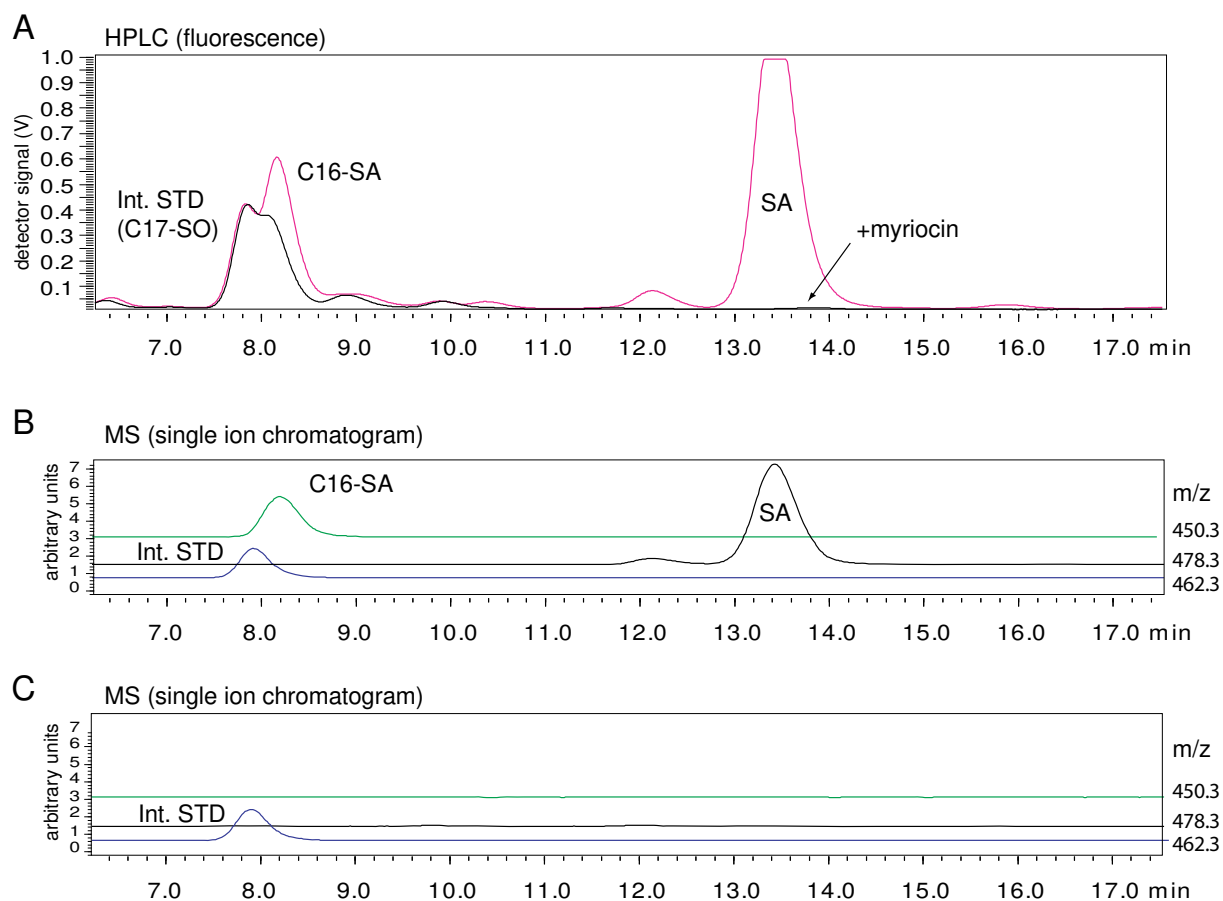


Fig. 1

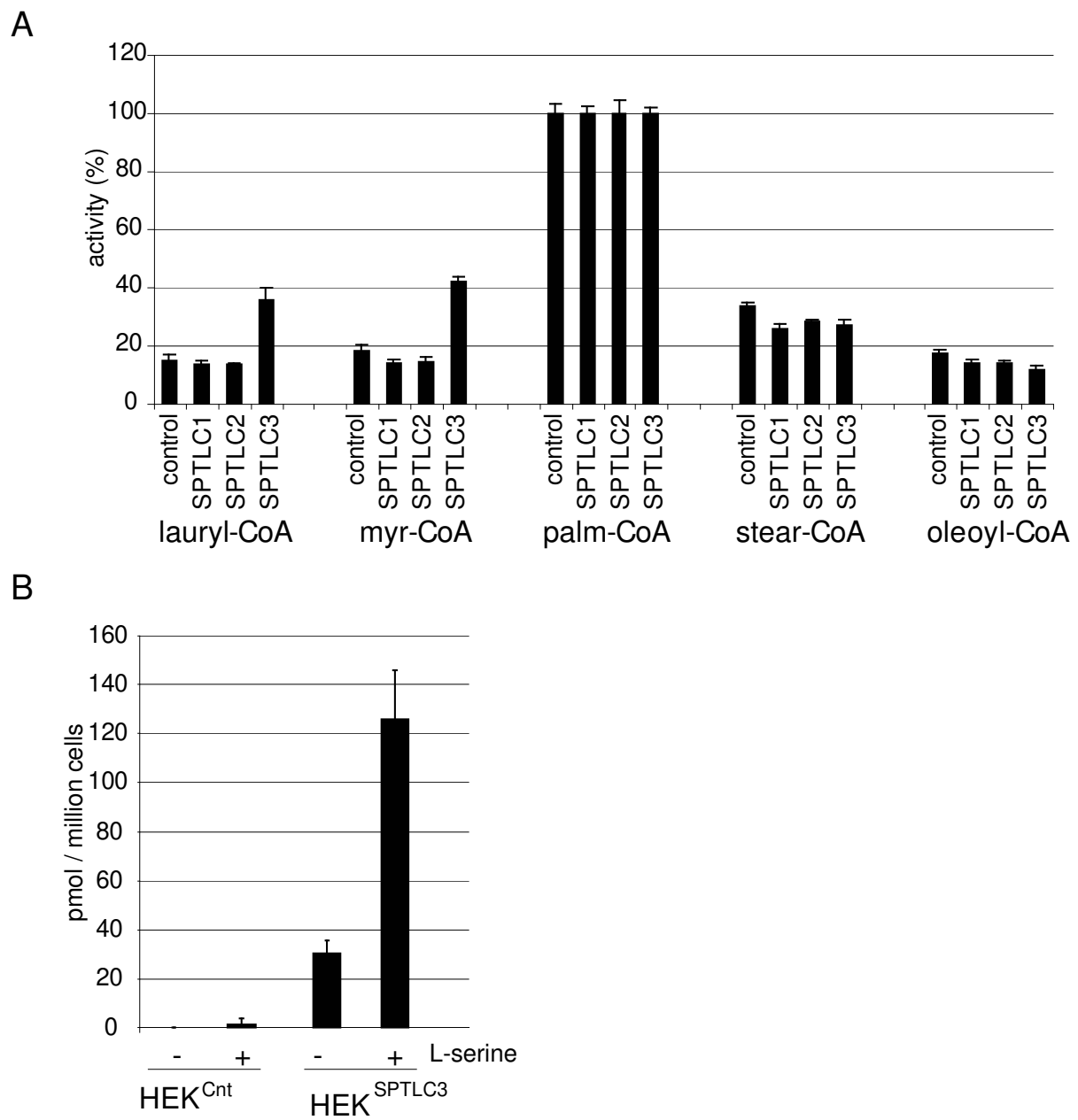


Fig. 2

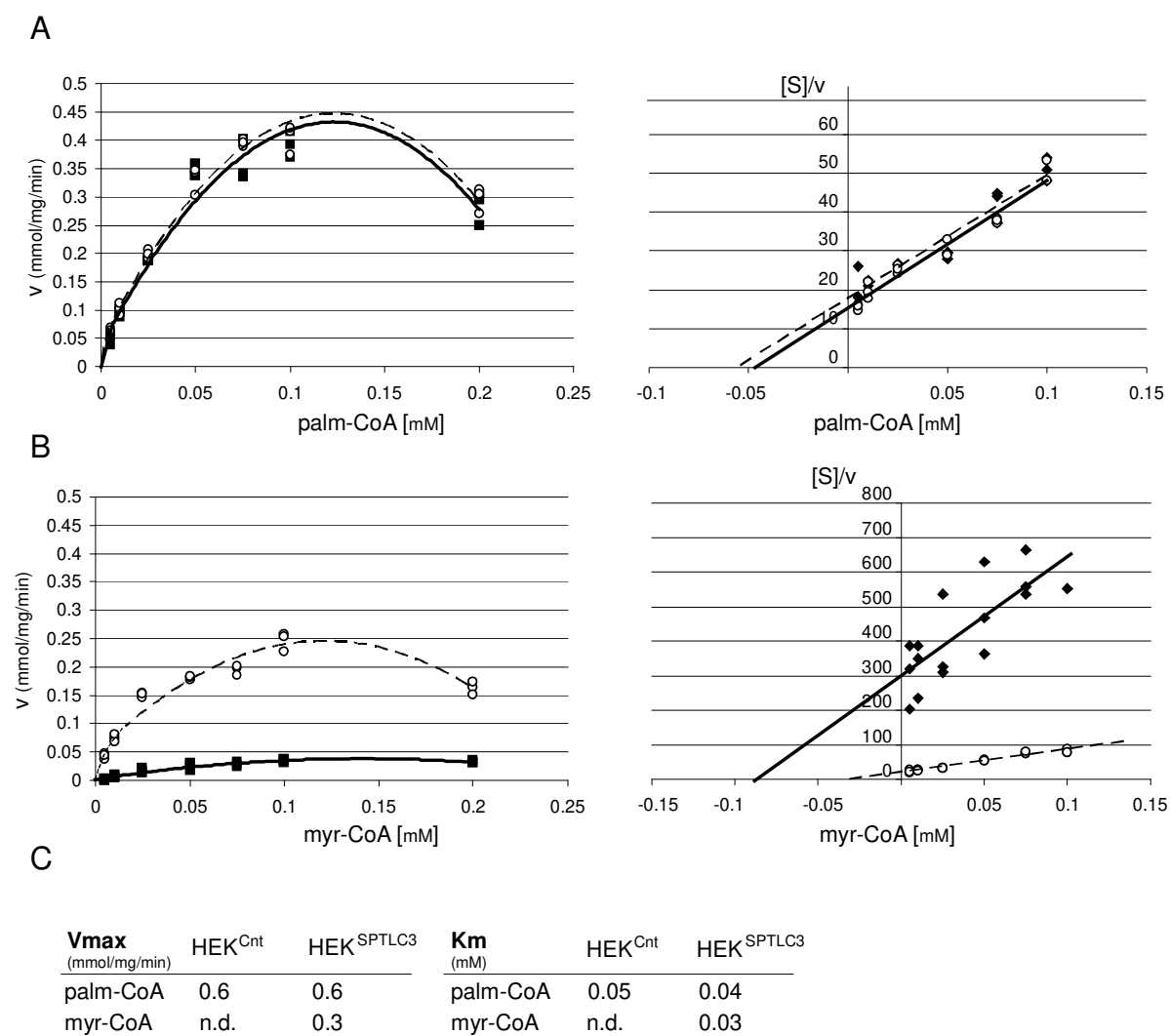


Fig. 3

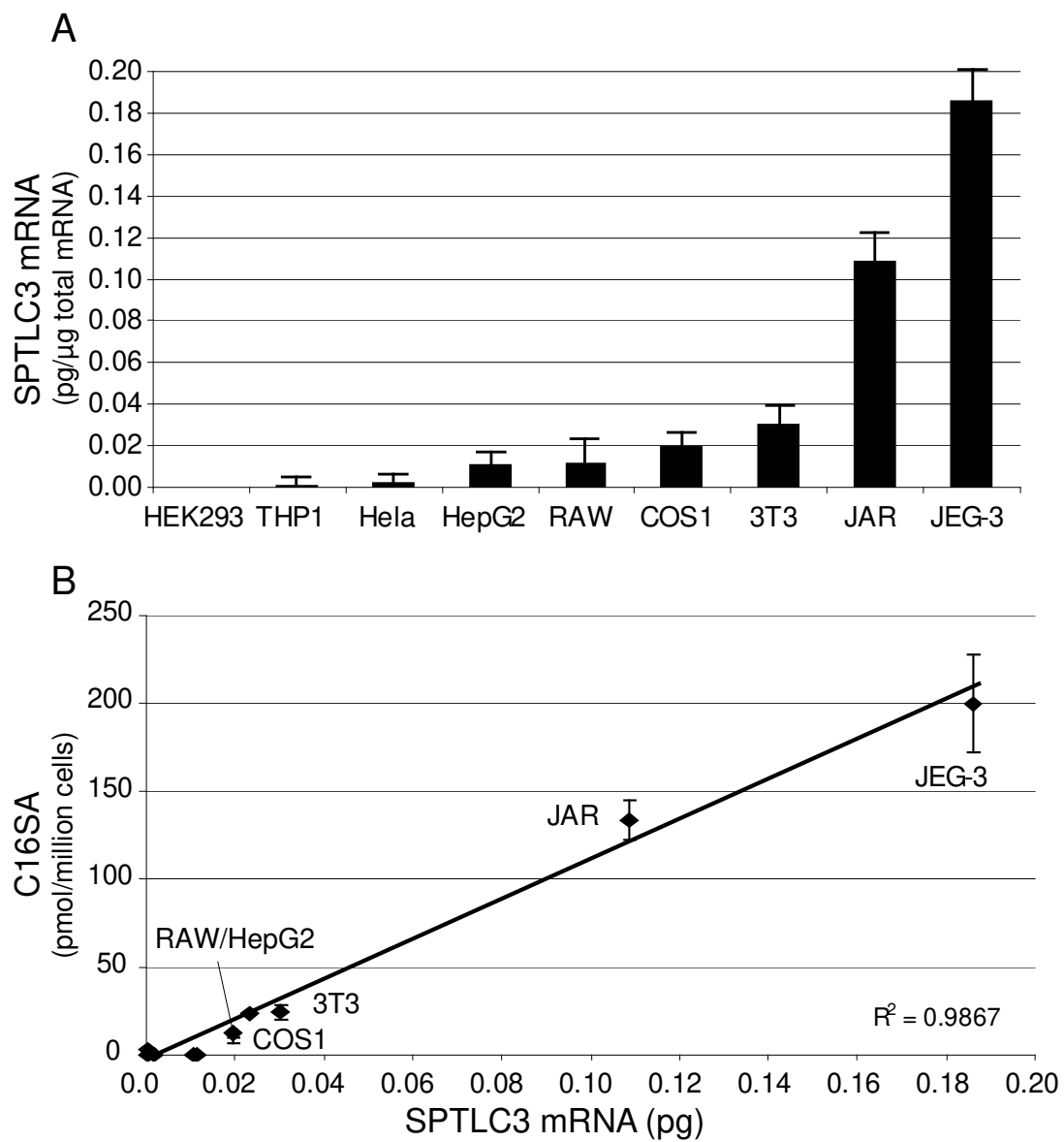
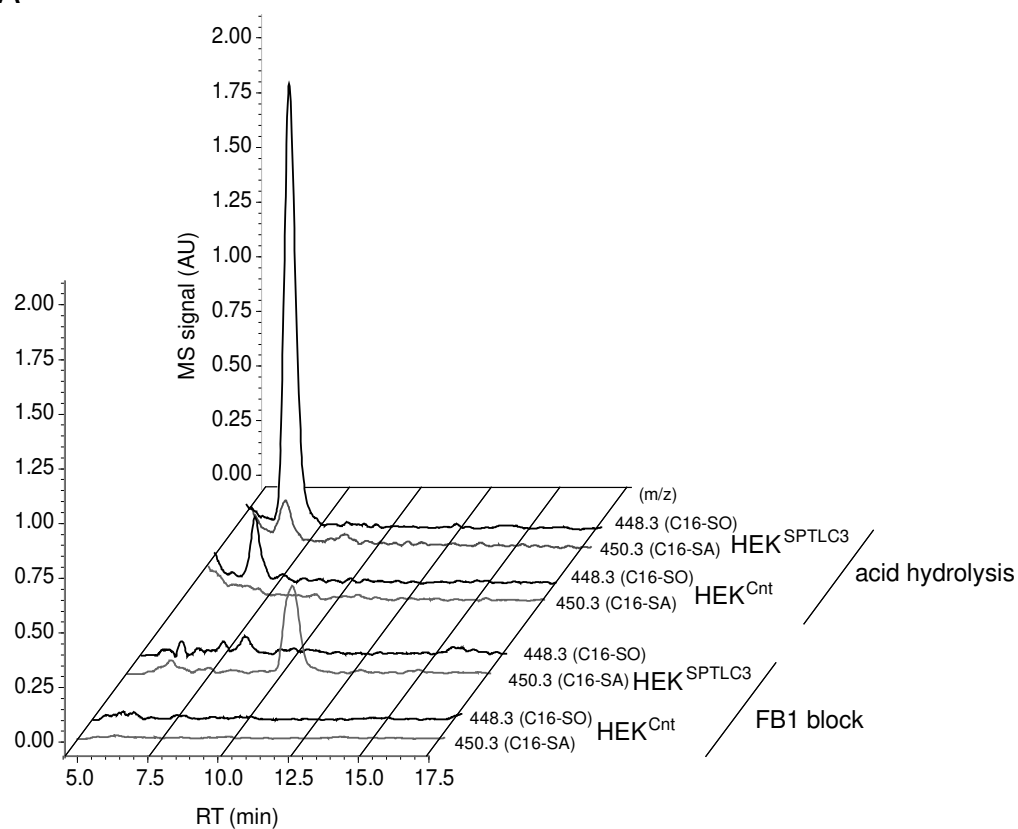
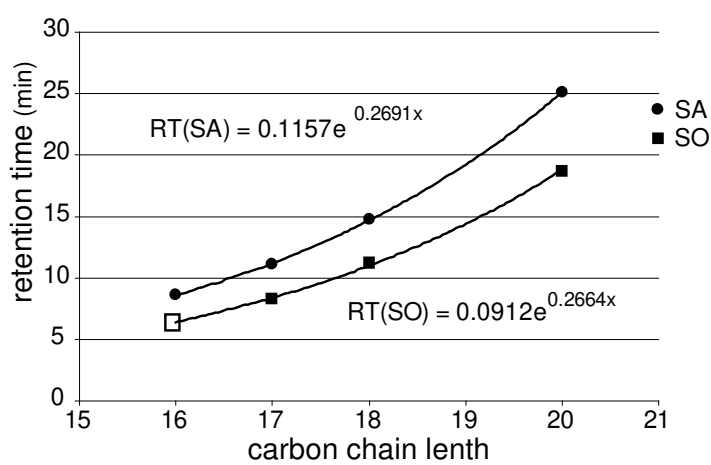


Fig. 4

A



B



C

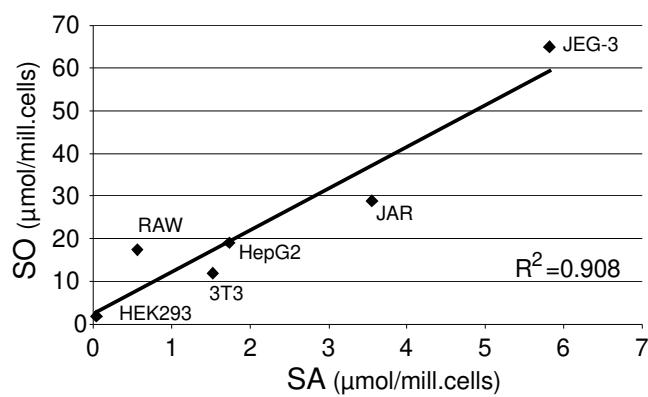


Fig. 5

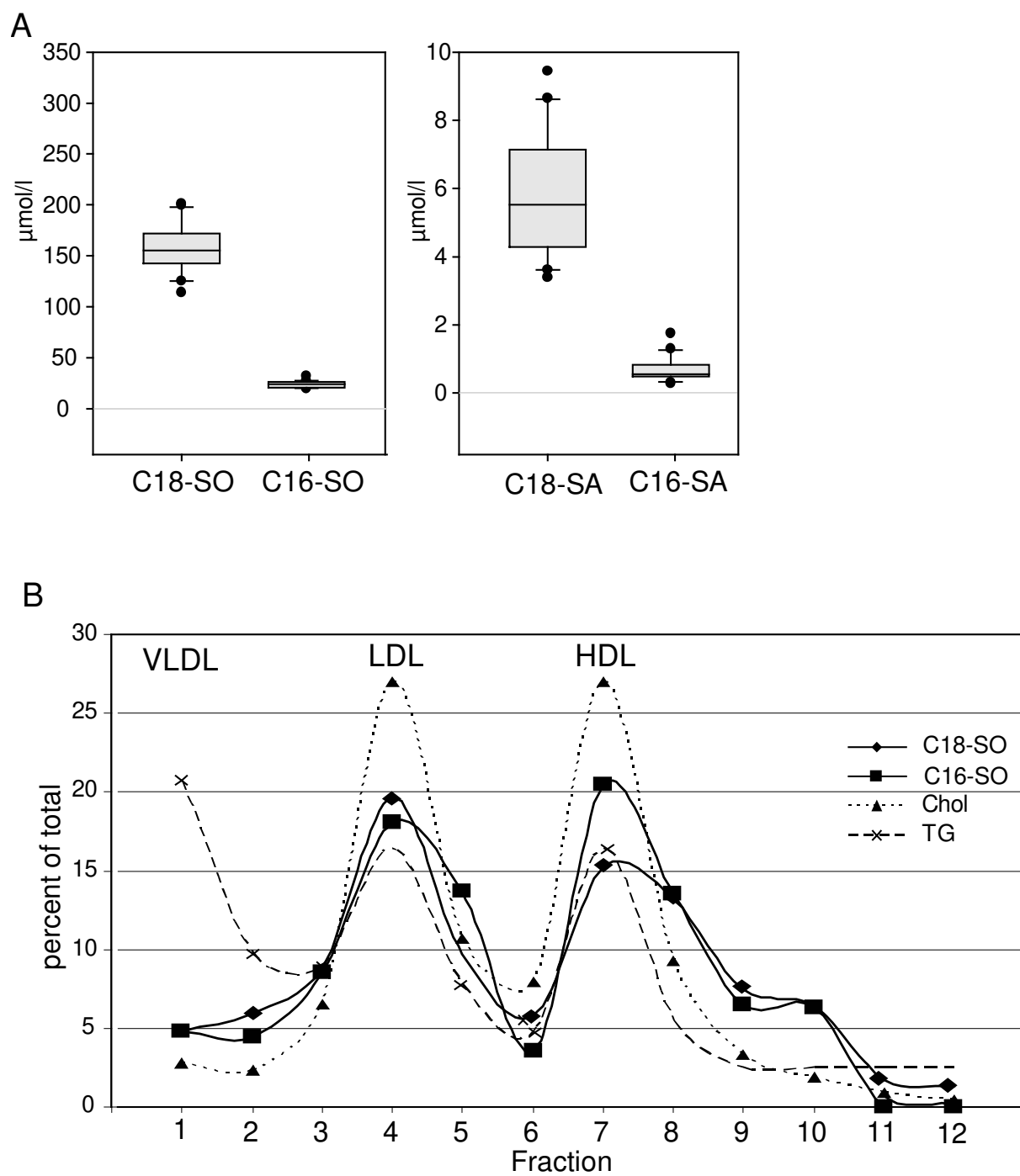


Fig. 6